Vanadium Oxide Supported on Al-modified Titania Nanotubes for Oxidative Dehydrogenation of Propane

Mojtaba Saei Moghaddam and Jafar Towfighi*

Department of Chemical Engineering, Tarbiat Modares University, Tehran, Iran.

(Received 2017.06.18, Accepted 2017.09.02)

Abstract

In this study, characterization of vanadia supported on Al-modified titania nanotubes (TiNTs) synthe-sized by the alkaline hydrothermal treatment of TiO2 powders has been reported. A promising catalyst for oxidative dehydrogenation (ODH) of propane was prepared via the incipient wetness impregnation method. The morphology and crystalline structure of TiNTs were characterized by transmission elec-tron microscopy (TEM) and X-ray diffraction (XRD). TiNTs provided large specific surface areas of about 408m2/gr and 1.603cm3/gr for pore volume. Rapid sintering and anatase to rutile phase transformation occurred in presence of vanadia in the catalysts at high calcination temperature. Al-promoted TiNTs considerably inhibited the loss of surface area so that a superior catalytic activity was observed in the ODH of propane along with amelioration of structural properties. The results showed 49.7% increase in propane conversion and 22.6% increase in propylene production at 500oC for Al-modified catalyst.

Keywords

Aluminium;
Oxidative dehydrogenation;
Propylene;
Titania nanotubes;
Vanadium oxide catalysts.

1. Introduction

Producing propylene oxide, polypropylene, paints, and plastics by several petrochemical and polymer processes along with the growth of world demand for these products depends on propylene as a key component in this industry [1, 2]. Oxidative dehydrogenation (ODH) of propane as a process for propylene production has received great attention in recent years. The advantages of this process include: (1) elimination of thermodynamic limitation, (2) low energy consumption, and (3) inhabitation of catalyst regeneration cycles. On the other hand, the simultaneous attendance of the propylene and propane in the reaction zone has been reported as the major obstacle in ODH process in the literature [3-6]. The catalytic systems based on vanadia are promising catalysts for the partial oxidation of hydrocarbons, especially at low loading of vanadium not exceeding a monolayer. They have been widely studied in ODH processes. It has been reported that the vanadia catalysts with coverage near the monolayer are the most active and selective catalysts, since they confine the formation of secondary oxygenated reaction products [7-9]. Vanadium oxides have been used as an active compo-

* Corresponding Author.
Tel./Fax: +982182883311
Email: towfighi@modares.ac.ir (J. Towfighi)

nent to MgO, γ-Al_2O_3, SiO_2, and TiO_2 [9-12]. Among all the reported catalytic systems, vanadium catalytic systems supported on TiO_2 have been found as the active and selective ones for selective catalytic oxidation and reduction reactions [10-14]. However, the main drawbacks associated with Titania are its lack of abrasion resistance, relatively rapid sintering, and low surface area that occurs at high temperatures [13-15].

Recently, several research groups have reported other active phases such as Pt-nanocrystals, WO_x, and Au-Rh. decorated on Titania Nanotubes (TiNTs), which are used for various chemical reactions with good results. TiNTs are highly active in propane ODH due to the large specific surface area and nano-scale structures, which increase the potential of reactive zone for the reaction. However, TiNTs suffer from low thermal stability. This obstacle can be tackled by modification of physico-chemical properties of TiNTs through doping with various species as promoters [16-20]. Furthermore, Reddy et al. [21] reported titania-based mixed oxide support with alumina and silica that had high surface area and thermally stable support. De Leon et al. [22] reported good thermal stability of their catalyst support in the presence of aluminum.

This study investigates employing modified TiNTs as support for vanadium oxide based catalysts to improve their thermal stability. Effects of the addition of aluminum to the support will also be discussed. Finally, morphology and catalytic performance of the prepared catalysts in oxidative dehydrogenation of propane are reported.

2. Experimental

2.1. Synthesis and modification of Titania nanotubes

TiNTs were synthesized [1] as follows: 2.1gr of commercial Degussa P25 powder was used as precursor, mixed with 200mL of 10M aqueous solution of NaOH in a perfluoroalkoxy (PFA) bottle. In this step, 1% (w/w) aluminum nitrate nonhydrate was dispersed in the mixture and stirred for 30min to synthesize Al-modified TiNTs. Then, the resultant solution was poured into Teflon-lined stainless steel autoclave up to 80% filling ratio of internal volume and kept at 140°C under autogenous pressure for 24h in an oven. Subsequently, it was cooled down to ambient temperature. After the hydrothermal synthesis, discharge from PFA bottle, centrifugation, and acid washing by the 0.1M dilute solution of HNO_3 for several times, pH value of the rising solution reached about 1. The resultant white precipitate was repeatedly washed with abundant deionized water to reduce Na content with ion-exchange process until the pH value of supernatant approached 7. Finally, the sediment was dried at 110°C for 24h in the oven.

2.2. Elaboration of the catalysts

The incipient wetness impregnation procedure was used to elaborate the two kinds of catalysts (modified and unmodified) containing 5wt% vanadium. Predetermined amounts of oxalic acid and ammonium metavanadate (molar ratio=2) were added to the specified deionized water according to the total pore volume of the supports. Then, it was stirred at 70°C after observing a dark blue (puke) solution. The calcined synthesized support was mixed into it. After the formation of a paste, the obtained samples were aged for about 5h, followed by drying at 110°C for 24h in the oven. The resulting samples were calcined in static air at 500°C. These prepared catalysts were termed VT and VALT. The one with 5wt% V_2O_5 supported on AL-modified titanate nanotubes was referred to as VALT.

2.3. Characterization

X-ray diffraction (XRD) of the prepared samples was performed with a Philips PW1800 diffractometer system utilizing Kα radiation from Cu target (λ=1.5418 Å). The diffraction intensity was measured over an angular range of $5^\circ < 2\theta < 70^\circ$ with 2θ step of 0.04° and a count time of 2 seconds per point.

To determine the morphology of the prepared samples, TEM measurement was done by employing transmission electron microscope "JEOL" JEM-2100 (200kv) equipped with an analytical system for energy dispersive X-ray spectrometry (EDX).

The specific surface areas (S_{BET}) of the prepared fresh and spent samples were determined from the Nitrogen adsorption-desorption isotherms using the Brunauer-Emmett-Teller (BET) mul-

tipoint equation. The apparatus used for the studies was a BELSORP Mini II analyzer.

The Raman spectroscopy was performed using a Bruker spectrophotometer (SENTERRA (2009)) equipped with high-energy laser diodes and a CCD detector (Andorf). A 785nm diode laser operated at 25mW was used for excitation. All spectra were recorded at a 2cm^{-1} resolution.

2.4. Catalytic tests

The catalytic tests for oxidative dehydrogenation of propane were performed in a fixed-bed downflow micro reactor with external diameter of 8mm and wall thickness of 1mm at atmosphere pressure. The reactor was heated in an electric furnace with a k-type thermocouple. In a blank run at 500^{o}C, the catalytic activity of the reactor full-packed with quartz wool was verified to be negligible. Typically, the flow rate of reactants was controlled at oxygen/propane molar ratio of 1 and in a total flow rate of 100ml.min^{-1} using calibrated mass flow controls (sevenstar). The mixing was done before contact with the catalyst.

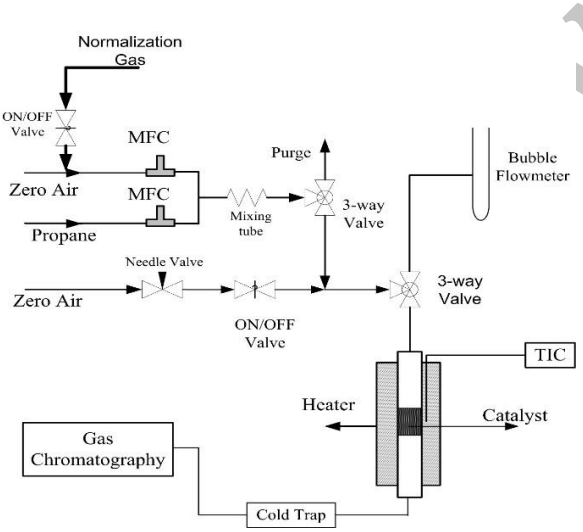

Figure 1. Schematic diagram of experimental setup

For each test, 100mg of catalyst was used. The catalyst was homogenously diluted with 100mg silicon carbide. The prepared samples were held on a plug of quartz wool. The catalysts were activated at 300^{o}C for 30min under zero air flow (20ml.min^{-1}) and the catalytic activity was determined at 300-500^{o}C by steps of 50^{o}C. After 30min, at each temperature, a sample of outlet gas mixture was extracted and analyzed online using Varian CP-3800 gas chromatograph. The results were presented as C_3H_8 conversion and selectivity toward C_3H_6 was calculated on a carbon atom basis. The molar yield of C_3H_6 was determined as the product of the C_3H_8 conversion and C_3H_6 selectivity. Carbon balance for all catalytic tests was established and found to be between ± 5%. A schematic diagram of experimental setup is shown in Fig. 1.

$$Propane\ Conversion = \frac{\sum_i (n_i \times C_i)_{products}}{3 \times n_{propane}}$$

$$Propylene\ Selectivity = \frac{3 \times n_{propylene}}{\sum_i (n_i \times C_i)_{products}}$$

Yield of propylene production = propane conversion × propylene selectivity

where n_i is the moles of component "i" and C_i represents the number of carbon atoms of component "i".

3. Results and Discussion

In order to investigate phase structure of the prepared samples, x-ray diffraction experiment was performed. The XRD pattern presented in Fig. 2(TiO_2-Degussa) indicates that the raw TiO_2 used as starting material for synthesis of TiNTs was fine anatase composition in the major phase diffraction peaks at 2θ =25.3^{o}, 36.8^{o}, 38^{o}, 48.1^{o}, 53.8^{o}, 55.1^{o}, and 62^{o} that corresponded to (1 0 1), (1 0 3), (0 0 4), (2 0 0), (1 0 5), (2 1 1), and (2 1 3) planes, respectively (JCPDS: 21-1272).

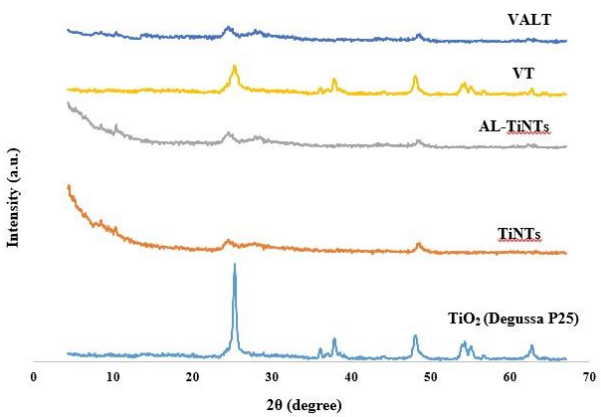

Figure 2. XRD patterns for all prepared samples

After alkali hydrothermal treatment followed by ion-exchange, the anatase phase of Degussa P25

was transformed into TiNTs. XRD pattern indicates 3 broad peaks, as shown in Fig. 2(TiNTs and AL-TiNTs) at 2θ =8.5°, 24.5°, and 48.6°, which correspond to (0 0 1), (0 0 3), and (0 2 0) planes, respectively, which may be assigned to $H_2Ti_5O_{11}.H_2O$ (JCPDS: 44-0131). The absence of aluminum species diffraction lines in Fig. 2(AL-TiNTs) may be due to the fine dispersion. More precisely, weak peak of $Na_2Ti_3O_7$ could be observed at 10°, which indicates that the crystallization did not occur completely because of the low protonated degree during acid washing step. This diffraction peak around 10° corresponds to the interlayer spacing between titanate sheets [23-26].

Fig. 2(VT and VALT) shows the XRD patterns of the catalysts containing vanadia. According to the results of Kootenaei et al. [27], the absence of characteristic peaks for vanadia are expressed through tiny vanadia crystals with concentrations and/or sizes outside the detection capacity of diffractometer or very fine dispersion of vanadia species on TiNTs. Various vanadia species can be detected according to the synthesis conditions of catalysts, type of the support, and the amount of vanadia loading. Lopez Nieto et al. [28] reported that the required molecules of vanadia for each cm^2 of support surface was 4.98 $\times 10^{14}$ to achieve a complete coverage. Higher loading tends to develop a crystalline phase. Hydrogen titanate nanotubes in the VALT sample demonstrate stronger peaks. Since the catalysts preparation conditions, especially calcination period in 500°C, led to collapse of TiNTs in VT catalyst and in the presence of vanadia, rapid sintering and anatase to rutile phase transformation occurred. However, some of TiNTs in AL-modified catalysts collapsed and others were reshaped to different nanostructures during the calcination at 500°C under static air. Therefore, AL had significant role in the thermal stability of titania nanostructures, because the intensity of diffraction peak around 8.5° corresponding to them rarely changed. In addition, AL modification led to hindering the anatase to rutile phase transformation upon vanadia decoration in VALT catalyst.

The TEM approach was performed in order to determine the morphology of TiNTs. Fig. 3 displays the transmission electron microscopy image of TiNTs; it can be seen that numerous randomly garbled open-ended tubular structures were produced. According to the surface morphology of supports, addition of AL to the TiNTs obviously affected thermal stability in the calcination treatment at 500°C under static air, and some TiNTs and nanostructures remained in compromise with the pure TiNTs, which completely collapsed. The supports were analyzed by EDX to study the surface composition of elements (Figs. 4 and 5). The results revealed the presence of Na in both synthesized supports because of the low protonated degree during acid washing step, which was in line with XRD results; furthermore, they proved the presence of AL in AL-TiNTs.

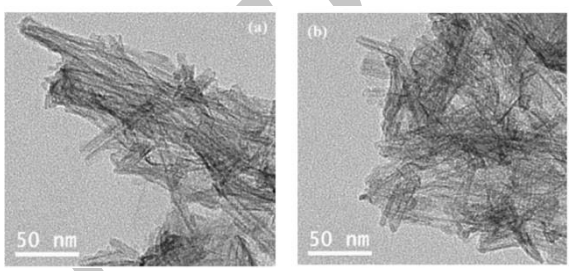

Figure 3. Transmission electron microscopy images of synthesized (a) TiNTs and (b) AL-TiNTs supports

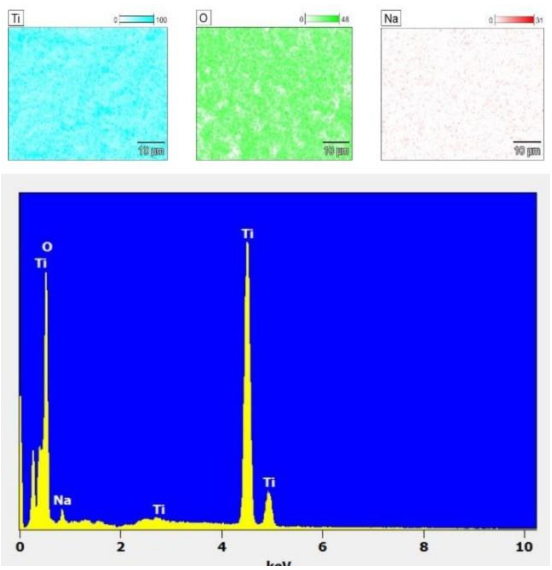

Figure 4. EDX dot mapping analysis of synthesized TiNTs

Table 1 lists the quantitative values of specific surface area and the pore volume for all prepared samples obtained by the representative N_2 absorption-desorption experiment. It can be noted that the specific surface area of TiNTs calculated using BET equation in N_2 isotherm significantly

increased from 52m²/gr to 408m²/gr for the sample before the hydrothermal treatment. The measured pore volume of TiNTs increased markedly to 1.603cm³/gr, which was much larger than that of TiO_2 precursor by a factor of about 5. That may be due to the formation of hollow-tubular structure by TiO_2 nanoparticles. Slight decreases in specific surface area and pore volume were founded for ALTiNTs sample and aluminum loading was responsible for these changes. However, the specific surface area for the catalysts calcined at 500°C significantly decreased due to the aggregation. However, the presence of aluminum had an important effect on the dehydration caused by heat treatment, as previously mentioned by XRD (see Fig. 2). Therefore, the specific surface area of VALT catalyst (97m²/gr**)** increased by about 30% from support (Al-TiNTs) in comparison with VT catalyst (78m²/gr), which had lower specific surface area than the pure TiNTs.

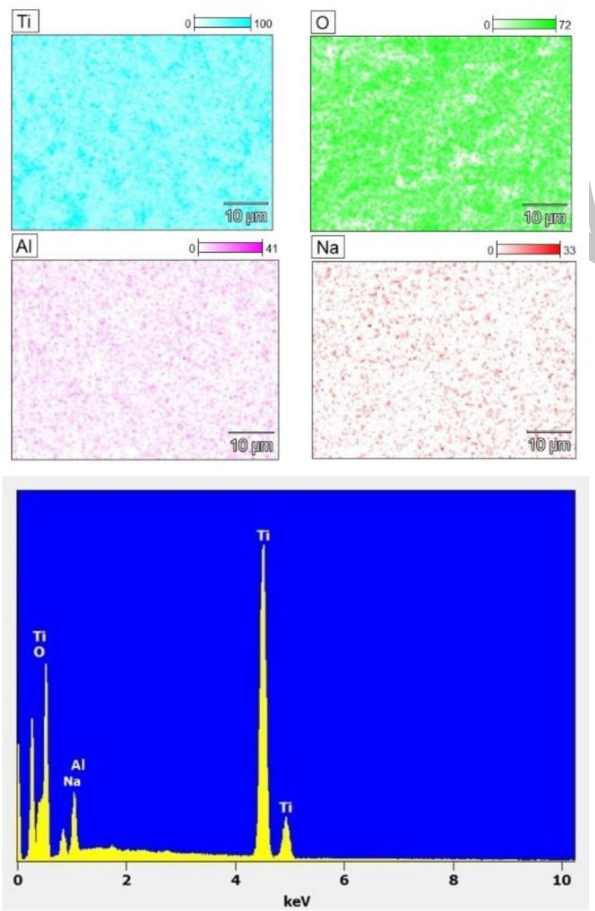

Figure 5. EDX dot mapping analysis of synthesized AL-TiNTs

Table 1. Values of specific surface area and pore volume for all prepared samples

Samples	a_s (m²/gr)	V_p (cm³/gr)
TiO_2 (Degussa P25)	52	0.351
TiNTs	408	1.603
Al-TiNTs	332	1.165
VT	78	0.732
VALT	97	0.856

Since Raman spectroscopy can supply the catalytic molecular structural data in various environmental conditions, it is a very versatile characterization test for the supported metal oxides [29]. The Raman spectra of TiNTs after acid treatment, followed by ion-exchange process, are presented in Fig. 6(a), which include two main characteristic peaks at 275 and 455cm⁻¹ along with other clear less intense peaks at 195, 393, 673, 838, 903, and 923cm⁻¹. Anatase active bands are 144, 200, 400, 505, 640, and 796cm⁻¹, by which two weak bands at 195 and 393cm⁻¹ are detected [30-32].

The indexation of the peaks in the Raman spectra of TiNTs is notably challenging. Recently, Toledo et al. [33] reported the broad peaks at 145,192, 278, 380, 450, 645, 700, 830, and 903cm⁻¹ for similar titanate nanotubes. Clearly, the bands at 145, 192, and 640cm⁻¹ are related to titania, proposing a combination of titanium oxide phases, that is, anatase and TiNTs are present. The peaks at 455 and 673cm⁻¹ are assigned to Ti–O–Ti vibration and the band at 903cm⁻¹ is related to Ti–O–Na vibrations in the interlayer zones of TiNTs [29, 32]. Further, new research has reported Raman bands at 266, 448, 668, and 917cm⁻¹ for TiNTs [33].

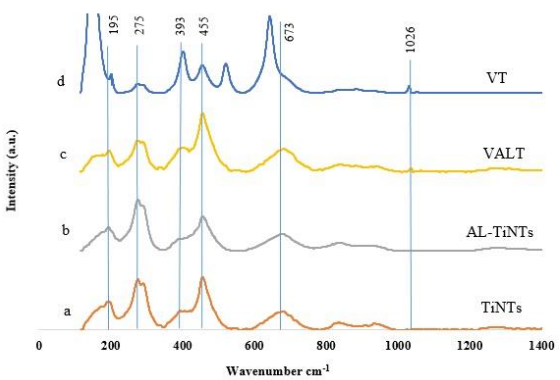

Figure 6. Raman spectra of TiNTs after acid treatment of AL-TiNTs, VALT, and VT samples

Qian et al. [34] reported that the band at 266cm^{-1} was attributed to Ti-O-H bonds. It was suggested that these bonds had substantial role in formation and stability of TiNTs. Nevertheless, in Raman spectra of our prepared sample, the vibrating bands at 266, 450, and 668 cm^{-1} are shifted to 275, 455, and 673cm^{-1}, respectively. The peak intensity at 903cm^{-1} is insignificant due to the low Na content remaining after acid washing. Waches et al. [29] reported that the band at ~923cm^{-1} corresponded to an overtone of the 453–458 band, unlike the previous literature that assigned it to Na-O-Ti.

A survey of literature reveals that the surface vanadium oxide in the titanium oxide and crystalline V_2O_5 has two forms of vanadia, which are present in Raman characterization of freshly prepared V_2O_5 supported TiO_2 catalyst. Raman bands at 141, 191, 281, 406, 526, 697, and 997cm^{-1} are ascribed to the bulk of V_2O_5 for V_2O_5 supported TiO_2 catalyst. The major peak of V_2O_5 crystalline is at 997cm^{-1} and is related to V=O stretching mode [35].

The Raman spectra of hydrated surface vanadium oxide over TiO_2 consist of two relatively broad bands at 795 and 930cm^{-1}, which are placed with a singlet band at 1025cm^{-1} in dehydration procedure. It is shown that anatase to rutile transformation begins by heat temperature treatment, leading to decrease in the surface vanadia. However, as Fig. 6(c and d) shows, the hollow-tubular structure of TiO_2 is significantly destroyed for the catalysts calcinated at 500^{o}C under static air. This result is related to the aggregation. The presence of aluminum has important effect on the dehydration caused by heat treatment, leading to the collapse of VT catalyst. The band at 266cm^{-1} is attributed to Ti-O-H bonds, which has an insignificant intensity compared to that in the VALT catalyst. This bonds have substantial role in formation and stability of TiNTs. During high-temperature calcination, the destruction of tube-like structure two Ti-OH bond release H_2O and a Ti-O-Ti bond which tend to formation of anatase phase [36]. This is in agreement with the BET analysis.

The catalytic performance of both samples in ODH of propane has been evaluated. The obtained results in temperature range of 300-500^{o}C are depicted in Fig. 7. In the ODH of propane reaction system, CO, CO_2, and H_2O were also produced in addition to propylene as desired products. Moreover, traces of methane and ethylene were also formed at higher temperatures as cracking products.

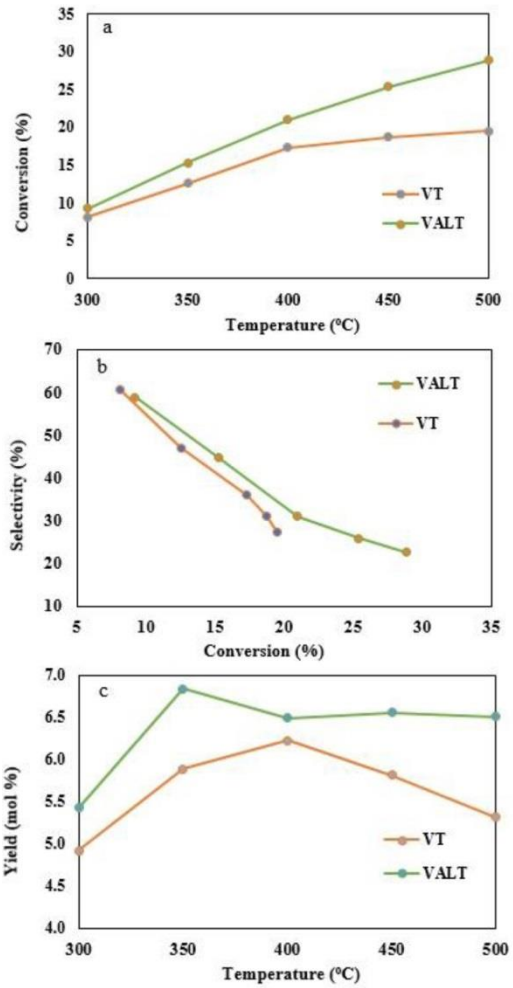

Figure 7. The catalytic performance for ODH of propane over VALT and VT catalysts

As shown in Fig. 7, the conversion of propane increases with increase in temperature and the selectivity toward the propylene decreases due to the emergence of carbon oxides. A general trend indicates the trade-off relationship between the propane conversion and the propylene selectivity. These results are in agreement with the suggested parallel-consecutive reaction, such as the ODH of propane reaction. Other researchers have also reported the low propylene selectivity for vanadia catalysts supported by titania nanoshapes [19, 27].

As shown in Fig. 7(a), the values of propane conversion as functions of reaction temperature for 2

samples are presented. The conversion levels are different on both samples, indicating the higher activity of the VALT catalyst with aluminum content. It seems that VALT catalyst consists more active catalytic sites than VT catalyst does. This behavior must be attributed to the decrease in specific surface area due to the rapid sintering, which occurs at temperatures above 400°C, as reported by Chunyi et al. [36]. This could be in line with the specific surface area measured via BET analysis. It should be noted that the specific surface area of VT is lower than that of VALT, which contains the same amount of vanadium oxide. Comparing BET surface area, the surface area decreases slightly during the calcination treatment due the presence of aluminum. Al has important influence on the thermal stability and the inhibition of anatase to rutile phase transformation in the sample.

Nevertheless, the propylene selectivity versus propane conversion profile remains the same, demonstrating that relative concentration of surface vanadia species and amount of crystalline vanadium oxide phase as different active sites remain the same. Since all VO_x species are highly dispersed on the surface of catalysts, as illustrated by the XRD and Raman studies, there is inconsiderable variation of propylene selectivity among the catalysts when compared under iso-conversion.

As seen in Fig. 7(c), the molar yield of propylene production as a function of reaction temperature for both samples is presented. The results confirm 49.7% increase in the propane conversion and 22.6% increase in propylene production yield at 500°C for Al-modified catalyst due to the desired physicochemical properties compared to VT catalyst.

4. Conclusion

Hydrothermal synthesized TiNTs provided the sample with high specific surface area and larger pore volume in comparison with the TiO_2 precursor. However, the catalyst with vanadia had low surface area due to rapid sintering and anatase to rutile phase transformation. Characterization methods revealed that doping aluminum in the support had obvious effect on the texture property, crystal structure upon heat treatment, and catalytic activity in the oxidative dehydrogenation of propane to propylene. 49.7% increase in propane conversion and 22.6% increase in propylene production yield at 500°C were observed for VALT catalyst compared to VT catalyst, which could be attributed to the presence of aluminum in the synthesized support.

References

[1] Putra, M.D., Al-Zahrani, S.M. and Abasaeed, A.E. (2011). "Oxidative dehydrogenation of propane to propylene over Al_2O_3-supported Sr–V–Mo catalysts." *Catalysis Communications*, Vol. 14, pp. 107-110.

[2] Sun, X., Ding, Y., Zhang, B., Huang, R. and Su, D.S. (2015). "New insights into the oxidative dehydrogenation of propane on borate-modified nanodiamond." *Chemical Communicatioms*, Vol. 51, pp. 9145-8.

[3] Putra, M.D., Al-Zahrani, S.M. and Abasaeed, A.E. (2012). "Oxidehydrogenation of propane to propylene over Sr–V–Mo catalysts: Effects of reaction temperature and space time." *Journal of Industrial and Engineering Chemistry*, Vol. 18, pp. 1153-1156.

[4] Siahvashi, A., Chesterfield, D. and Adesina, A.A. (2013). "Nonoxidative and Oxidative Propane Dehydrogenation over Bimetallic Mo–Ni/Al_2O_3 Catalyst." *Industrial & Engineering Chemistry Research*, Vol. 52, pp. 4017-4026.

[5] Ma, F., Chen, S., Zhou, H., Li, Y. and Lu, W. (2014). "Revealing the ameliorating effect of chromium oxide on a carbon nanotube catalyst in propane oxidative dehydrogenation." *RSC Advance*, Vol. 4, pp. 40776-40781.

[6] Chen, S., Ma, F., Xu, A., Wang, L., Chen, F. and Lu, W. (2014). "Study on the structure, acidic properties of V–Zr nanocrystal catalysts in oxidative dehydrogenation of propane." *Applied Surface Science*, Vol. 289, pp. 316-325.

[7] Löfberg, A., Giornelli, T., Paul S. and Bordes-Richard, E. (2011). "Catalytic coatings for structured supports and reactors: VOx/TiO_2 catalyst coated on stainless steel in the oxidative dehydrogenation of propane." *Applied Catalysis A: General*, Vol. 391, pp. 43-51.

[8] Fattahi, M., Kazemeini, M., Khorasheh, F. and Rashidi, A.M. (2013). "Vanadium pentoxide catalyst over carbon-based nanomaterials for the

oxidative dehydrogenation of propane." *Industrial & Engineering Chemistry Research*, Vol. 52, pp. 16128-16141.

[9] Rozanska, X., Fortrie, R. and Sauer, J. (2014). "Size-dependent catalytic activity of supported vanadium oxide species: oxidative dehydrogenation of propane." *Journal of the American Chemical Society*, Vol. 136, pp. 7751-7761.

[10] Banares, M. and Khatib, S. (2004). "Structure-activity relationships in alumina-supported molybdena-vanadia catalysts for propane oxidative dehydrogenation." *Catalysis Today*, Vol. 96, pp. 251-257.

[11] Zhang, J., Wang, Y., Jin, Z., Wu, Z. and Zhang, Z. (2008). "Visible-light photocatalytic behavior of two different N-doped TiO_2." *Applied Surface Science*, Vol. 254, pp. 4462-4466.

[12] Oliva, C., Cappelli, S., Rossetti, I., Ballarini, N., Cavani, F. and Forni, L. (2009). "EPR enlightening some aspects of propane ODH over VOx–SiO_2 and VOx–Al_2O_3." *Chemical Engineering Journal*, Vol. 154, pp. 131-136.

[13] Chakraborty, S., Nayak, S.C. and Deo, G. (2015). "TiO_2/SiO_2 supported vanadia catalysts for the ODH of propane." *Catalysis Today,* Vol. 254, pp. 62-71.

[14] Wang, C., Chen, J. G., Xing, T., Liu, Z. T., Liu, Z.W. and Jiang, J. (2015). "Vanadium Oxide Supported on Titanosilicates for the Oxidative Dehydrogenation of n-Butane." *Industrial & Engineering Chemistry Research*, Vol. 54, pp. 3602-3610.

[15] Reddy, B.M., Lakshmanan, P., Loridant, S., Yamada, Y., Kobayashi, T. and López-Cartes, C. (2006). "Structural Characterization and Oxidative Dehydrogenation Activity of V_2O_5/Ce x Zr1-x O_2/SiO_2 Catalysts." *The Journal of Physical Chemistry B*, Vol. 110, pp. 9140-9147.

[16] Cortés Corberán., V. (2009). "Nanostructured Oxide Catalysts for Oxidative Activation of Alkanes." *Topics in Catalysis*, Vol. 52, pp. 962-969.

[17] Shee, D. and Deo, G. (2009). "Adsorption and ODH reaction of alkane on sol–gel synthesized TiO_2–WO_3 supported vanadium oxide catalysts: In situ DRIFT and structure–reactivity study." *Journal of Molecular Catalysis A: Chemical*, Vol. 308, pp. 46-55.

[18] Lei, Y., Mehmood, F., Lee, S., Greeley, J., Lee, B. and Seifert S. (2010). "Increased silver activity for direct propylene epoxidation via subnanometer size effects." *Science*, Vol. 328, pp. 224-8.

[19] Kraemer, S., Rondinone, A.J., Tsai, Y.T., Schwartz, V.S., Overbury, H. and Idrobo, J.C. (2016). "Oxidative dehydrogenation of isobutane over vanadia catalysts supported by titania nanoshapes." *Catalysis Today*, Vol. 263, pp. 84-90.

[20] Rischard, J., Antinori, C., Maier, L. and Deutschmann, O. (2016). "Oxidative dehydrogenation of n-butane to butadiene with Mo-V-MgO catalysts in a two-zone fluidized bed reactor." *Applied Catalysis A: General*, Vol. 511, pp. 23-30.

[21] Reddy, B.M., Rao, K.N., Reddy, G.K. and Bharali, P. (2006). "Characterization and catalytic activity of V_2O_5/Al_2O_3-TiO_2 for selective oxidation of 4-methylanisole." *Journal of Molecular Catalysis A: Chemical*, Vol. 253, pp. 44-51.

[22] De León, M.A., De Los Santos, C., Latrónica, L.A., Cesio, M., Volzone, C. and Castiglioni , J. (2014). "High catalytic activity at low temperature in oxidative dehydrogenation of propane with Cr–Al pillared clay." *Chemical Engineering Journal*, Vol. 241, pp. 336-343.

[23] Wang, W., Zhang, J., Huang, H., Wu, Z. and Zhang, Z. (2008). "Surface-modification and characterization of H-titanate nanotube." C*olloids and Surfaces A: Physicochemical and Engineering Aspects*, Vol. 317, pp. 270-276.

[24] Fen, L.B., Han, T.K., Nee, N.M., Ang, B.C. and Johan, M.R. (2011). "Physico-chemical properties of titania nanotubes synthesized via hydrothermal and annealing treatment." *Applied Surface Science*, Vol. 258, pp. 431-435.

[25] Ou, H. and Lo, S. (2007). "Review of titania nanotubes synthesized via the hydrothermal treatment: Fabrication, modification, and application." *Separation and Purification Technology*, Vol. 58, pp. 179-191.

[26] Liu, J., Fu, Y., Sun, Q. and Shen, J. (2008). "TiO_2 nanotubes supported V2O5 for the selective oxidation of methanol to dimethoxymethane." *Microporous and Mesoporous Materials*, Vol. 116, pp. 614-621.

[27] Kootenaei, A.H.S., Towfighi, J., Khodadadi, J.A. and Mortazavi, Y. (2014). "Stability and catalytic performance of vanadia supported on

nanostructured titania catalyst in oxidative dehydrogenation of propane." *Applied Surface Science*, Vol. 298, pp. 26-35.

[28] Concepción, P., Nieto, J.L. and Pérez-Pariente. J. (1994). "Oxidative dehydrogenation of ethane on a magnesium-vanadium aluminophosphate (MgVAPO-5) catalyst." *Catalysis letters*, Vol. 28, pp. 9-15.

[29] Kim, S.J., Yun, Y.U., Oh, H.J., Hong, S.H., Roberts, C.A. and Routray, K. (2009). "Characterization of hydrothermally prepared titanate nanotube powders by ambient and in situ Raman spectroscopy." *The Journal of Physical Chemistry Letters*, Vol. 1, pp. 130-135.

[30] Shi, L., Cao, L., Liu, W., Su, G., Gao, R. and Zhao, Y. (2014). "A study on partially protonated titanate nanotubes: Enhanced thermal stability and improved photocatalytic activity." *Ceramics International*, Vol. 40, pp. 4717-4723.

[31] Gannoun, C., Turki, A., Kochkar, H., Delaigle, R., Eloy, P. and Ghorbel, A. (2014). "Elaboration and characterization of sulfated and unsulfated V_2O_5/TiO_2 nanotubes catalysts for chlorobenzene total oxidation." *Applied Catalysis B: Environmental*, Vol. 147, pp. 58-64.

[32] Cortés-Jácome, M.A., Ferrat-Torres, G.L., Ortiz, F.F., Angeles-Chávez, C., López-Salinas, E. and Escobar J. (2007). "In situ thermo-Raman study of titanium oxide nanotubes." *Catalysis Today*, Vol. 126, pp. 248-255.

[33] Ma, R., Fukuda, K., Sasaki, T., Osada, M. and Bando, Y. (2005). "Structural features of titanate nanotubes/nanobelts revealed by Raman, X-ray absorption fine structure and electron diffraction characterizations." *The Journal of Physical Chemistry B*, Vol. 109, pp. 6210-6214.

[34] Qian, L., Du, Z.L., Yang, S.Y. and Jin, Z.S. (2005). "Raman study of titania nanotube by soft chemical process." *Journal of Molecular Structure*, Vol. 749, pp. 103-107.

[35] Stencel, J.M. (1989). *Raman spectroscopy for catalysis*, Springer.

[36] Wang, G., Wu, W., Zhu, X., Sun, Y., Li, C. and Shan, H. (2014). "Effect of calcination temperature on isobutane dehydrogenation over Mo/MgAl2O4 catalysts." *Catalysis Communications*, Vol. 56, pp. 119-122.